Chemical Physics 66 (1982) 465–470
North-Holland Publishing Company

PHOTOFRAGMENTATION OF $SnCl_2$ AT 193 nm

N.J.A. VAN VEEN *, G.N.A. VAN VEEN, M.S. DE VRIES ** and A.E. DE VRIES
FOM-Institute for Atomic and Molecular Physics, 1098 SJ Amsterdam, The Netherlands

Received 6 November 1981

Using photofragment spectroscopy the time of flight spectra and angular distributions for SnCl fragments, Sn and Cl atoms from the fragmentation of $SnCl_2$ have been measured at 193 nm. From the time of flight it was found that dissociation takes place into SnCl ($X\,^2\Pi$) and Cl(^2P) and that the SnCl fragment is highly vibrationally excited. To account for this effect we propose a mechanism, in which the upper potential surface has a saddle point at a greater Sn–Cl_2 distance than the ground state. The angular distribution exhibits an anisotropy parameter $\beta = 0.21$. A model was developed, based on a charge transfer from the p nonbonding orbitals on the Cl atoms to the p_x orbital on the Sn atom. The model predicts that $A_1 \rightarrow B_2$ transitions dominate over $A_1 \rightarrow A_1$ transitions and that $A_1 \rightarrow B_1$ transitions are negligible in good agreement with the experimental observations.

1. Introduction

Tin dihalides have been studied through the years by several investigators [1–4]. Of all tin dihalides, $SnCl_2$ probably is the most thoroughly studied as it is the only tin dihalide that yields predominantly the monomeric species in the gas phase [5]. Most of these investigations were confined to the identification of the absorption continua. The ultraviolet absorption cross sections were measured by Maya [6a], and show a pronounced double headed peak around 200 nm, which is the subject of this study. According to Maya light absorption in this region might lead to dissociation into SnCl ($A'\,^2\Sigma^+$) and Cl(^2P). Neujmin [3] studied the absorption of $SnCl_2$ at 185 nm and found subsequent emission in the regions 380–350 nm and 330–285 nm which he attributed to SnCl($A\,^2\Delta \rightarrow X\,^2\Pi$) transitions and SnCl($B\,^2\Sigma \rightarrow X\,^2\Pi$) transitions respectively. In principle this would open up the possibility for an efficient production of SnCl in an electronically excited state with complete population inversion. Using the photofragment spectroscopy technique, pioneered by Busch and Wilson [7] combined with the measurement of the angular distribution as started by Bersohn and co-workers [8], we will show that at 193 nm none of the formerly mentioned processes is dominant but that at this wavelength the major dissociation route is into SnCl($^2\Pi$) and Cl(^2P), ruling out the possibility of an ArF (193 nm) pumped SnCl laser. Furthermore, we have developed a simple model, which is based on a charge transfer from a nonbonding p on the Cl atom to the p_x orbital on the Sn atom. This model allows for an explanation of the experimentally observed angular distribution of photofragments as mainly due to a parallel transition.

2. Experimental setup

The apparatus used for the experiments has been extensively described elsewhere [9]. Therefore only a brief description will be given here. A molecular beam, a laser and a neutral detector are mutually perpendicular. The chambers which contain the beam source, the interaction region and the detector are pumped differentially. The $SnCl_2$ molecular beam originates from a stainless steel oven with an orifice of 2 mm diameter operated at a temperature of about 600 K. This temperature corresponds to a steady salt pressure of

* Present address: Columbia University, Department of Chemistry, New York, NY 10027, USA.
** Present address: University of California, Department of Chemistry, St. Barbara, Ca 93106, USA.

0301-0104/82/0000–0000/$02.75

200 Pa [10]. The laser beam originates from a pulsed rare gas halide laser whose light is polarized by passing it through a stack polarizer consisting of 10 parallel plates of suprasil quartz placed at Brewsters angle. The polarization of the light is rotated by a zero order half wave plate.

After traveling over a flight path of 100 mm the photofragments are detected by a quadrupole mass spectrometer with an electron bombardment ionizer. Ions are counted as a function of time after each laser shot by a multichannel scaler with 512 channels with a minimum dwell time of 1.5 μs. The multichannel scaler is coupled to a PDP 11/70 by means of Camac and a display enables online observation of the development of the experiment.

3. Principle of the experiment

The photofragmentation technique is based upon the measurement of velocity and angular distribution of photofragments. Velocity distributions of the formed fragments yield information about the dissociation channels, dissociation energies and in the case of polyatomic molecules about the transfer of excess energy into rotational and vibrational energy of the fragments. The angular distributions are indicative of the type of transition taking place. In a photofragment experiment the angular distribution of photofragments in the center of mass is given by [11]

$$I(\theta) = \tfrac{1}{4}\pi[1 + 2\beta P_2(\cos\theta)] , \qquad (1)$$

where $I(\theta)$ is the relative intensity at center of mass angle θ, β is the anisotropy parameter and $P_2(\cos\theta)$ is the second Legendre polynomial in $\cos\theta$. It can be shown that for fast dissociation the anisotropy parameter can be written as [12]:

$$\beta = P_2(\cos\phi) , \qquad (2)$$

where ϕ is the angle between the transition dipole moment $\overline{\mu_{if}}$ and the c.m. recoil direction $\overline{u}$.

4. Results and discussion

4.1. The time of flight spectrum

Time of flight spectra were measured for SnCl molecules, Sn and Cl atoms. These are shown in fig. 1a, 1b and 1c. The spectra for the Sn atoms and the SnCl molecules look identical. Therefore we believe the Sn signal to arise from dissociative ionization of SnCl molecules in the electron bombardment ionizer [13]. After correction for the transit time through the quadrupole mass spectrometer it turns out that the SnCl molecules and the Cl atoms have the same translational momentum and therefore arise from the same dissociation process.

From the energetics of the absorption, Maya [6a] suggested that the state to which excitation takes place at 193 nm relates in the diabatic limit to $SnCl(A'\,^2\Sigma^+) + Cl(^2P)$. This however requires a dissociation energy of D_0 ($SnCl_2 \rightarrow$ ground state SnCl + Cl) + excitation energy $SnCl(A'\,^2\Sigma^+ \leftarrow X\,^2\Pi_{1/2}) = 3.9 + 2.4 = 6.3$ eV [3,14]. This is inconsistent with the experimental time of flight spectra from which we find that on the average 1.7 eV is carried away by the fragments as translational energy instead of the 0.1 eV as would be the result of the process indicated by Maya. We therefore infer that dissociation takes place into $SnCl(X\,^2\Pi)$ and $Cl(^2P)$. This is in agreement with a more recent paper by Maya [6b]. In this paper the search for fluo-

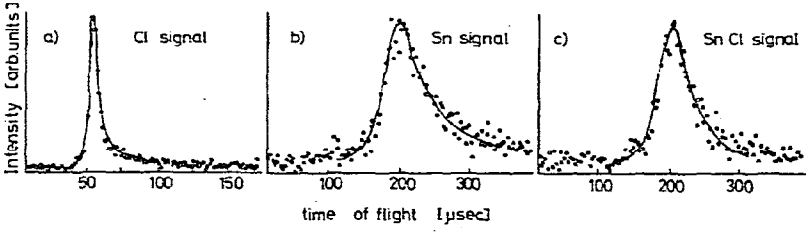

Fig. 1. Time of flight spectra for Cl and Sn atoms and SnCl molecules from the photofragmentation of $SnCl_2$ at 193 nm.

rescence from $SnCl_2$ as a result of photoexcitation by ≈200 nm is reported to give negative results. Although both fragments must be in their ground electronic states there are four possible pairs of fragment fine structure states ($^2\Pi_{1/2}$, $^2P_{3/2}$), ($^2\Pi_{1/2}$, $^2P_{1/2}$), ($^2\Pi_{3/2}$, $^2P_{3/2}$) and ($^2\Pi_{3/2}$, $^2P_{1/2}$) lying at 0, 881, 2356 and 3237 cm^{-1} above the lowest possible energy. Thus the vibrational and rotational energy of SnCl is between 0.4 and 0.8 eV. A dynamic model as the spectator model [15] permits an estimate of the amount of energy transferred into rotational energy of the diatomic fragment,

$$E_{rot} = (M_{Cl}/M_{SnCl})^2 \sin^2 \theta_0 E_{avl} = 0.05 E_{avl}, \qquad (3)$$

where E_{avl} is the available energy and θ_0 is the Cl–Sn–Cl bond angle. The mass dependent prefactor limits the transfer into rotational energy to about 0.1 eV. Because of the fact that the bond angle is almost 90°, the spectator model does not allow energy to be transferred into vibrational energy. Also a sudden model [16] in which the SnCl equilibrium distance changes instantly from the value it has in the molecule to the value of the SnCl fragment cannot account for the large energy transfer. In fig. 2 we have sketched a possible potential energy surface of the excited molecule which may lead to highly vibrationally excited fragments. In the following section we show that the excited orbital is symmetrically antibonding with respect to both Cl atoms. So it may be expected that as a first result of the excitation the Sn–Cl_2 equilibrium distance increases. As there is not enough energy for a three-body dissociation, which would require 7.5 eV [17], the system moves through the "saddle" and at the opposite turning point it rolls back and down into either one of the potential wells of the SnCl molecule. In order to put about 0.5 eV of vibrational energy in the SnCl oscillator the saddle point has to be extended by about 0.01 nm with respect to the equilibrium position of the well in the ground state of the $SnCl_2$ molecule.

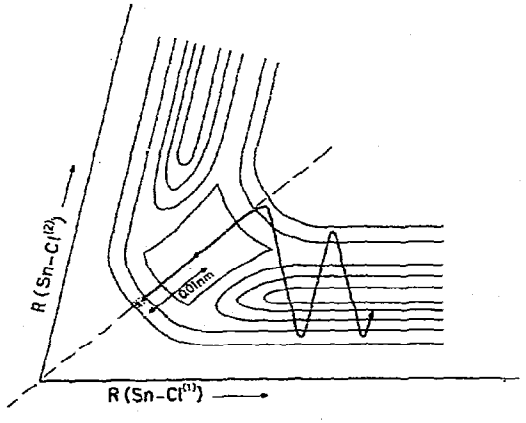

Fig. 2. Schematic drawing of the proposed potential energy surface for the excited state of $SnCl_2$. The axes have been drawn with the so-called "skew" angle. The dashed ellips denotes the part of phase space from where the dissociative trajectories start. A possible trajectory is indicated by the thick solid line.

4.2. The angular distribution

The angular distributions of Cl atoms and SnCl fragments are both shown in fig. 3a and 3b. Both exhibit the same anisotropy factor $\beta = 0.21 \pm 0.01$. If it is assumed that dissociation is fast with respect to molecular rotation then this relates to a characteristic angle of 46.5° ± 0.4° between the transition dipole moment and the dissociation direction. This indicates that the transition dipole moment is not perpendicular to the molecular plane as in that case the anisotropy factor would be –0.5, but rather in the molecular plane itself. It is, however, inconclusive whether it is directed along the Cl–Cl axis ($A_1 \rightarrow B_2$ transition) or along the C_2 axis ($A_1 \rightarrow A_1$ transition) as the Cl–Sn–Cl bond angle in the ground state is presumably 95° [18] resulting in characteristic angles of 42.5° and 47.5° respectively.

In the following section we will develop a simple

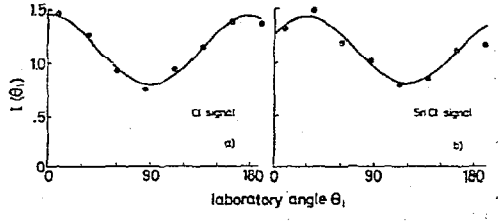

Fig. 3. Angular distributions for Cl atoms and SnCl molecules from the photofragmentation of $SnCl_2$ at 193 nm. The solid line is a least-squares fit to the data of the form $I(\theta) = 1 + 2\beta P_2(\theta_l - \theta_0)$. The fit yields for the Cl signal $\beta = 0.21 \pm 0.01$, $\theta_0 = 0°$ and for the SnCl signal $\beta = 0.21 \pm 0.01$ and $\theta_0 = 14°$.

charge transfer model pioneered by Mulliken for H_2^+ [19] and by Zare and Herschbach for the alkali halides [20]. Hastie et al. [21] calculated the energy levels for the homologue molecule $GeCl_2$, using extended Hückel theory. As the orbital energies for Ge and Sn differ only by tenths of one eV [22] we believe the $GeCl_2$ MO scheme also to be appropriate for $SnCl_2$. From the scheme it can be seen that the photon energy of 6.4 eV fits between degenerate levels of nonbonding electrons located on the Cl atoms and a b_1 molecular orbital which is mainly built up from a p_x orbital on the Sn atom.

5. The model

In the following model calculations it is presumed for the sake of simplicity that the Cl–Sn–Cl bond angle is 90° and that the overlap between p orbitals located on different Cl atoms is zero. For the description of the symmetry group C_{2v} to which $SnCl_2$ belongs, we follow the recommendation by Mulliken [23] that b_1 is related to the x-direction which is perpendicular to the molecular plane, b_2 relates to the y-direction, aligned with the Cl–Cl axis and the z-axis is taken along the C_2 axis. There are three matrix elements that contribute to transitions to a b_1 molecular orbital;

(i) $\langle b_1|x|a_1\rangle$, (ii) $\langle b_1|y|a_2\rangle$, (iii) $\langle b_1|z|b_1\rangle$.

The final state orbital which has b_1 symmetry can be described as

$$\psi_f^{b_1} = C_1\,[|p_x^{Sn}\rangle - \alpha(|p_x^1\rangle + |p_x^2\rangle)]\,, \tag{4}$$

where the upper indices refer to the different Cl atoms. The a_1 molecular orbital is built up from two p orbitals on the Cl atoms whose axes are located in the plane of the molecule

$$\psi_i^{a_1} = 2^{-1/2}(|p_\pi^1\rangle + |p_\pi^2\rangle)\,. \tag{5}$$

In this molecular orbital we have neglected the p_z^{Sn} [21]. The a_2 orbital is made up from the p_x orbitals on the Cl atoms, comparable with the Π_g orbital in the Cl_2 molecule:

$$\psi_i^{a_2} = 2^{-1/2}(|p_x^1\rangle - |p_x^2\rangle)\,. \tag{6}$$

The b_1 orbital contains the symmetric combination of p_x orbitals, comparable with the Π_u orbital in the Cl_2 molecule, and a contribution from the p_x^{Sn} in order to make it orthogonal to the b_1 orbital representing the final state

$$\psi_i^{b_1} = C_2(|p_x^1\rangle + |p_x^2\rangle + \gamma|p_x^{Sn}\rangle)\,. \tag{7}$$

Normalization provides expressions for C_1 and C_2;

$$C_1 = (1 + 2\alpha^2 - 4\alpha S)^{-1/2}\,, \tag{8}$$

$$C_2 = (2 + 4\gamma S + \gamma^2)^{-1/2}\,, \tag{9}$$

where S stands for the overlap integral $\langle p_x^i|p_x^{Sn}\rangle$. From orthogonalization we find a relation between γ and α

$$\alpha = \frac{\gamma + 2S}{2 + 2\gamma S} \quad \text{or} \quad \gamma = \frac{2\alpha - 2S}{1 - 2\alpha S}\,. \tag{10}$$

We now can start with the evaluation of the matrix elements. The transition dipole moment in the x-direction yields:

$$\mu_x = e\langle\psi_f^{b_1}|x|\psi_i^{a_1}\rangle = 2^{-1/2}eC_1(2\alpha K)\,, \tag{11}$$

where K represents the two centre integral $\langle p_x^1|x|p_\pi^2\rangle$. As p_π^2 and the Cl–Cl direction are not perpendicular this contribution is not equal to zero. However, if we consider the big distance between the two Cl atoms of 6.5 a_0, [24], combined with the fact that a Slater type orbital representation for the 3p orbital on the Cl peaks at 1.04 a_0 [25], then it becomes obvious that the resulting matrix element is negligible.

The transition dipole moment in the y-direction results in

$$\mu_y = e\langle\psi_f^{b_1}|y|\psi_i^{a_2}\rangle = 2^{-1/2}eC_1(2D + 2\alpha B)\,, \tag{12}$$

if we take the origin in the center of the Cl–Cl axis then B represents half the Cl–Cl distance and D is the two-centre integral $\langle p_x^1|y|p_x^{Sn}\rangle$. In the same manner the transition dipole moment in the z-direction is

$$\mu_z = e\langle\psi_f^{b_1}|z|\psi_i^{b_1}\rangle = eC_1C_2\,[2E(1 - \alpha\gamma) + \gamma H]\,, \tag{13}$$

where H stands for the distance from the Sn atom to the Cl–Cl axis and E is the two centre integral $\langle p_x^1|z|p_x^{Sn}\rangle$.

Assuming a Cl–Sn–Cl bond angle of 90° we find that B equals H and that D equals E. Now it is possible to find the ratio of transition intensities polarized in the z-direction to those polarized in the y-direction;

$$R = \mu_z^2/\mu_y^2 = 2C_2^2\left[\frac{2E(1-\alpha\gamma)+\gamma H}{2E+2\alpha H}\right]^2. \qquad (14)$$

In order to make a fair estimate of the ratio R we have to make a reasonable guess of the magnitude of the two-centre integral E. An upper limit may be found from the crude approximation $\langle p_x^1|z|p_x^{Sn}\rangle = \frac{1}{2}S(\langle p_x^1|z|p_x^1\rangle + \langle p_x^{Sn}|z|p_x^{Sn}\rangle)$ [26] leading to the expression

$$E = 0.5\,HS\,\epsilon\,, \qquad (15)$$

where ϵ is a fit parameter with values ranging from zero to one. After substitution of (9), (10) and (15) in (14) one obtains the final expression for R:

$$R = \frac{2^{-1}}{(2+4\gamma S+\gamma^2)}\left[\frac{S\epsilon(2-\gamma^2)+2\gamma(1+\gamma S)}{S\epsilon(1+\gamma S)+(\gamma+2S)}\right]^2. \qquad (16)$$

This function is plotted in fig. 4 as a function of γ for several values of S with ϵ ranging from zero to one. A remarkable feature is that for any combination of variables, μ_y is greater than μ_z. Furthermore, the model shows that the ratio is only slightly dependent on ϵ and that in the limit of $\gamma \to 0$, μ_z^2 is negligible with respect to μ_y^2.

Hastie et al. [21] indicate that the b_1 excited state orbital is about 90% of a p_x orbital on the metal atom. This yields a value $R \leqslant 0.83$, the maximum being obtained for $S = 0$.

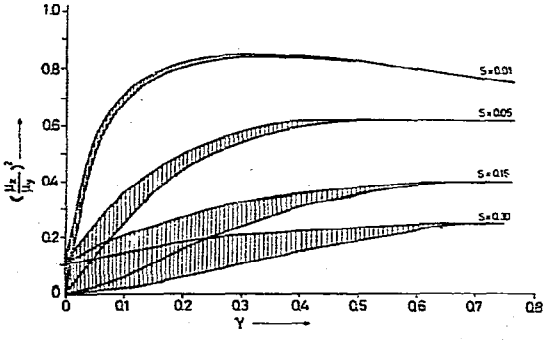

Fig. 4. Plot of the ratio $R = \mu_z^2/\mu_y^2$ as a function of the mixing parameter γ for several values of S with ϵ ranging from 0 to 1.

Although the model does not exclude transitions in the z-direction it indicates that transitions in the y-direction are preferred and that transitions in the x-direction can be neglected. Moreover in this model all calculations have been performed assuming a bond angle of 90°. From (12) and (13) it can be seen that the ratio R will decrease even more if the bond angle is increased to the accepted value of 95° [18].

6. Conclusion

The time of flight spectrum shows that $SnCl_2$ at 193 nm dissociates in $Cl(^2P)$ and a vibrationally hot $SnCl(^2\Pi)$ fragment. The transfer of available excess energy into rotational + vibrational energy of the SnCl molecule can be explained by an excited potential surface on which the SnCl distance is greater than in the $SnCl_2$ ground state. The angular distribution of fragments can be accounted for by simple model calculations which indicate that transitions in the y-direction are preferred to transitions in the z-direction. Moreover, the model shows that although it is symmetry allowed the transition intensity in the x-direction is negligible, in good agreement with the experimental findings.

Acknowledgement

We are greatly indebted to Professor Richard Bersohn and Dr. U.C. Klomp for many valuable discussions concerning this subject. The work described here is part of the research program of the Stichting voor Fundamenteel Onderzoek der Materie (Foundation for Fundamental Research on Matter) and was made possible by financial support from the Nederlandse Organisatie voor Zuiver-Wetenschappelijk Onderzoek (Netherlands Organization for the Advancement of Pure Research).

References

[1] D. Naegeli and H.B. Palmer, J. Mol. Spectry. 21 (1966) 325.
[2] G.A. Oldershaw and K. Robinson, J. Chem. Soc. A 19 (1971) 2963.

[3] H. Neujmin, Acta Physiochim. USSR 2 (1935) 595.
[4] R. Samuel, Rev. Mod. Phys. 18 (1946) 103.
[5] L. Andrews and D.L. Frederick, J. Am. Chem. Soc. 92 (1970) 775.
[6] (a) J. Maya, J. Chem. Phys. 67 (1977) 4976;
(b) J. Maya, Appl. Phys. Letters 32 (1978) 484.
[7] G.E. Busch and K.R. Wilson, Rev. Sci. Instr. 41 (1970) 1066.
[8] C. Jonah, P. Chandra and R. Bersohn, J. Chem. Phys. 55 (1971) 1903.
[9] M.S. de Vries, Thesis, University Amsterdam, The Netherlands (1980).
[10] C.R. Weast, ed., Handbook of chemistry and physics, 52nd Ed. (Chem. Rubber Co., Cleveland, 1971–72).
[11] R.N. Zare, Mol. Photochem. 4 (1972) 1.
[12] R. Bersohn and S.H. Lin, Advan. Chem. Phys. 16 (1969) 67.
[13] M. Kawasaki, S.J. Lee and R. Bersohn, J. Chem. Phys. 71 (1979) 1235.
[14] K.P. Huber and G. Herzberg, Constants of diatomic molecules (Van Nostrand, Princeton, 1979).
[15] B.H. Mahan, J. Chem. Phys. 52 (1970) 5221.
[16] A.D. Wilson and R.D. Levine, Mol. Phys. 27 (1974) 5221.
[17] A.S. Buchanan, D.J. Knowles and D.L. Swinger, J. Chem. Phys. 73 (1969) 4394.
[18] M.W. Lister and L.E. Sutton, Trans. Faraday Soc. 37 (1941) 406.
[19] R.S. Mulliken, J. Chem. Phys. 7 (1939) 1420.
[20] R.N. Zare and D.R. Herschbach, J. Mol. Spectry. 15 (1965) 462.
[21] J.W. Hastie, R.H. Hauge and J.L. Margrave, J. Mol. Spectry. 29 (1969) 512.
[22] C.E. Moore, Circ. N.B.S. 467, Vols. II–III (1952).
[23] R.S. Mulliken, J. Chem. Phys. 23 (1955) 1997.
[24] P.A. Ashikin, V.P. Spiridonov and A.N. Khodchenkov, Zh. Fiz. Khim. 32 (1958) 1679.
[25] P.O. Offenhartz, Atomic and molecular orbital theory (McGraw-Hill, New York, 1970).
[26] R.S. Mulliken, J. Chim. Phys. 46 (1949) 497.